Analytica Chimica Acta 1202 (2022) 339641

Contents lists available at ScienceDirect

Analytica Chimica Acta

journal homepage: www.elsevier.com/locate/aca

Sequential detection of dopamine and L-DOPA by a 2,3-dopa-dioxygenase from *Streptomyces sclerotialus*

Chia-Wen Chang [1], Yu-Hsuan Lin [1], Cheng-Han Tsai [1], Sivasankar Kulandaivel , Yi-Chun Yeh [*]

Department of Chemistry, National Taiwan Normal University, Taipei, 11677, Taiwan

HIGHLIGHTS

- A novel heat-stable enzyme was used in the development of a biosensor for the detection of L-dopa.
- Sequential detection of dopamine and L-DOPA was achieved with dual-fluorescence signals.
- The efficacy of the resulting sensor was evaluated using serum samples.
- Paper microfluidics modified with chitosan was applied to enhance sensitivity for fast and cost-effective analysis.

GRAPHICAL ABSTRACT

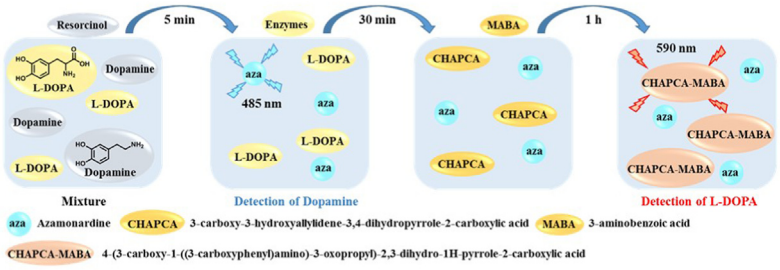

ARTICLE INFO

Article history:
Received 26 December 2021
Received in revised form
16 February 2022
Accepted 21 February 2022
Available online 1 March 2022

Keywords:
L-DOPA
Dopamine
Colorimetric biosensors
2,3-Dopa-dioxygenase
Pigment

ABSTRACT

A variety of enzyme-based colorimetric biosensors have been developed for clinical practice; however, these methods will only become cost-effective when they are able to process multiple samples with a high degree of sensitivity. In this study, a novel heat-stable enzyme, 2,3-dopa-dioxygenase from the thermophilic bacterium *Streptomyces sclerotialus* (SsDDO), was used in the development of a protein- and cell-based biosensor for the detection of L-DOPA for the first time. SsDDO catalyzes the oxidative cleavage of L-DOPA forms linear semialdehyde (AHMS) and cyclizes to a 3-carboxy-3-hydroxyallylidene-3,4-dihydropyrrole-2-carboxylic acid (CHAPCA). We next derivatized CHAPCA by reacting with 3-aminobenzoic acid (MABA) to yield a red-fluorescent pigment. Overall, the detection of L-DOPA via the red fluorescent signal can be completed in only 30 min. We also developed a sequential analysis method to detect the coexistence of dopamine and L-DOPA with a high degree of sensitivity using the dual-fluorescent signals to monitor the therapy of patients with Parkinson's disease treated with L-DOPA. The robustness and applicability of the system were further validated in serum. In addition, paper microfluidics modified with chitosan was applied for fast and cost-effective analysis of dopamine and L-DOPA in the mixed solutions.

* Corresponding author.
E-mail address: yichuny@ntnu.edu.tw (Y.-C. Yeh).
[1] These authors contributed equally to this work.

https://doi.org/10.1016/j.aca.2022.339641
0003-2670/

1. Introduction

Catecholamine neurotransmitters, including 3,4-dihydroxy-*l*-phenylalanine (L-DOPA), dopamine, epinephrine (Epi), and norepinephrine (NE) are regulated by emotional states, body movements, and cognitions [1–3]. For example, excessively high or low dopamine concentrations in the body can have adverse effects. Parkinson's disease and attention deficit disorder are both characterized by a lack of dopamine, whereas schizophrenia and ganglioglioma are associated with excess concentrations [4,5]. In clinical treatment, L-DOPA remains the most effective symptomatic treatment of Parkinson's disease, because it can cross the cerebrovascular barrier to be converted into dopamine through amino acid decarboxylase [6–9]. Thus, L-DOPA and dopamine concentrations must be carefully monitored in patients to avoid potential confounding effects of other related neurotransmitter systems [10–12]. However, a selectively discrimination between L-DOPA and structurally related dopamine remains a challenge.

Existing detection methods such as electrochemical systems [13–15], high-performance-liquid-chromatography (HPLC) [16,17], spectrophotometry [18,19], capillary electrophoresis [20,21] require expensive instruments and time-consuming pre-processing. Electrochemical sensors are also sensitive to compounds but a similar oxidation-reduction potential, such as urea or ascorbic acid, overlap with the characteristic peaks of catecholamine compounds that interfere with detection. In the presence of these compounds, L-DOPA concentrations cannot be accurately measured. Phase chromatography provides excellent specificity; however, the instruments are expensive and require operation by highly-skilled professionals. By contrast, colorimetric or fluorescent-based biosensors provide rapid detection with a high degree of specificity [22–26]. Dopa-dioxygenase (part of vicinal-oxygen-chelate (VOC) enzyme family) is crucial to the breakdown of catechol in various positions of catecholamine compounds [27–29]. In the current study, we established a novel enzyme, 2,3-dopa-dioxygenase from the thermophilic bacterium *Streptomyces sclerotialus* (SsDDO), to facilitate the generation of colorimetric/fluorescent probe for use in L-DOPA detection. The SsDDO enzyme converts L-DOPA into 3-carboxy-3-hydroxyallylidene-3,4-dihydropyrrole-2-carboxylic acid (CHAPCA), which has a characteristic absorption value at 414 nm [30]. When reacted with 3-aminobenzoic acid (MABA), CHAPCA undergoes a 1,4-addition reaction to produce a pigment with red fluorescence 4-(3-carboxy-1-((3-carboxyphenyl)amino)-3-oxopropyl)-2,3-dihydro-1H-pyrrole-2-carboxylic acid (CHAPCA-MABA). L-DOPA can then be detected via either absorption or fluorescent signal output. Selectivity tests on the SsDDO enzyme verified the stability and applicability of the enzyme system in the detection of L-DOPA in fetal bovine serum. In addition, we developed a stepwise reaction (Scheme 1) to sequentially detect both dopamine and L-DOPA. Dopamine was firstly reacted with resorcinol to produce azamonardine with cyan fluorescence [31–33]; L-DOPA reacts with the SsDDO enzyme and MABA to form CHAPCA-MABA with red fluorescent pigment. The dual fluorescence detection of cyan (azamonardine) and red (CHAPCA-MABA) fluorescence can then be used to detect dopamine and L-DOPA in mixed solution, respectively. Lastly, paper microfluidics modified with chitosan was applied for fast and cost-effective analysis of dopamine and L-DOPA in the mixed solutions.

2. Experimental section

2.1. Chemicals

The chemicals were purchased from ACROS, such as dopamine, L-DOPA, tyramine, ascorbic acid, norepinephrine, epinephrine, glutamic acid, and phenylalanine. The iron(II) sulfate, tryptophan, phenylethylamine were brought from Sigma-Aldrich. The glycine, isopropyl β-D-1-thiogalactopyranoside (IPTG), carbenicillin, and glycerol were obtained from Amresco. Tyrosine was purchased from Merck. Fetal Bovine Sera (FBS) and artificial urine were purchased from GE Healthcare Life Sciences, respectively; calcium chloride was purchased from Ferak Berlin GmbH. Magnesium sulfate was purchased from Fisher chemical.

2.2. Mass expression and purification of SsDDO protein

We transformed the plasmid (pYCY_1138) into *Escherichia coli* BL21 (*E.coli* BL21) and spread it evenly on a solid LB medium containing 50 μg/mL carbenicillin by cultivating it at 37 °C overnight. Bacterium strain was grown in LB medium at 37 °C and 250 rpm for 16–18 h. Diluted cultured bacterial solution was placed in 250 mL LB broth containing carbenicillin at a ratio of 1%, and was placed in a 37 °C incubator to cultivate until (OD_{600} = 0.4–0.6), after induction with 1 mM Isopropyl β-D-1-thiogalactopyranoside (IPTG). The induced bacterial solution was centrifuged at 9000 rpm for 5 min at 4 °C, and the supernatant was discarded. Target protein containing

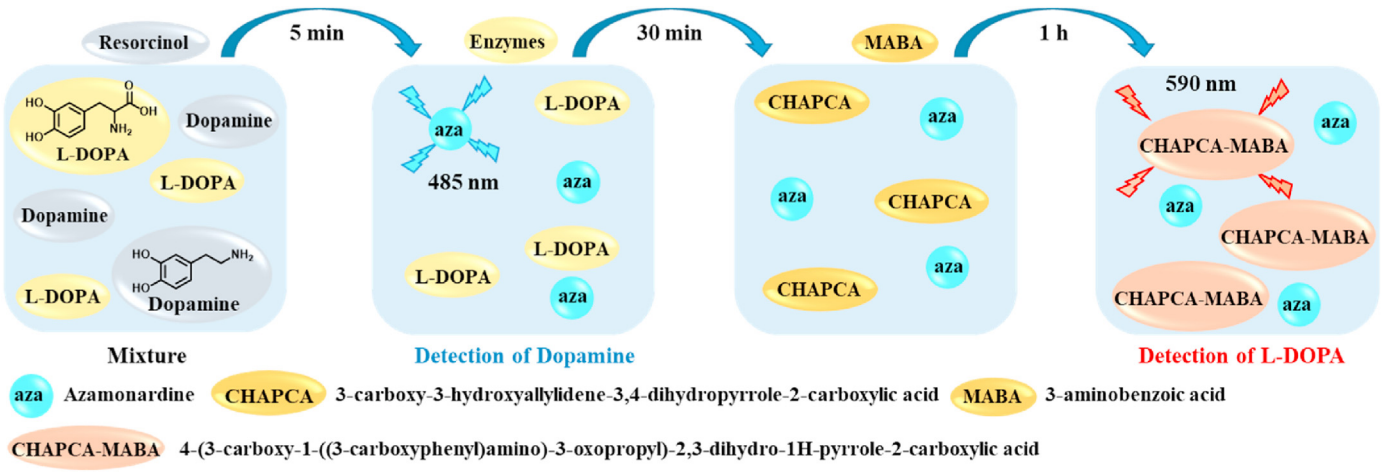

Scheme 1. A novel approach for the detection of dopamine and L-DOPA via a stepwise reaction. Resorcinol is used to detect dopamine, and *E. coli* cells expressing SsDDO were used to produce CHAPCA in the presence of L-DOPA. MABA was next reacted with CHAPCA to generate a red fluorescent pigment.

His-tag modification was purified using common protein purification protocols. The purified protein solution is dialyzed in phosphate buffer at 4 °C, and stored in refrigerator at 4 °C.

2.3. Interference study

The reaction condition containing sodium phosphate buffer (62.5 mM, pH 6.8) is the buffer solution for the SsDDO enzyme test. The reaction solution containing AA (10 mM), $FeSO_4$ (1 mM), 16.5 μM SsDDO, and 125 μM various catecholamines was used for the interference tests. The interference studies used the compounds with a similar structure to L-DOPA and common metabolites, such as dopamine (DA), epinephrine (Epi), norepinephrine (NE), phenethylamine (PEA), tyramine (tyramine), phenylalanine (Phe), tyrosine (Tyr), tryptophan (Trp), ascorbic acid (AA).

2.4. Enzyme kinetics

Substrates (L-DOPA and dopamine at 0, 100, 200, 400, 800, 1600, 2500, 3200 μM) were used to react with SsDDO for 10 min at room temperature, and the absorbance at 414 nm was measured with a 96-well plate reader. The molar absorption coefficient of CHAPCA ($\varepsilon = 30680\ M^{-1}cm^{-1}$), using Beer-Lambert law to obtain the volume molar concentration of CHAPCA, dividing it by the reaction time to get the initial reaction velocity (V_0), and the substrate of concentration and reaction rate into the Michaelis-Menten equation for fitting. After calculation, the K_M, kcat, and Vmax constants were obtained.

2.5. ESI-Q-TOF

Mass spectrometry was performed using electrospray ionization quadrupole time-of-flight mass spectrometry (ESI-Q-TOF). Analysis of CHAPCA and CHAPCA-MA were performed by infusion of samples into mass spectrometry. Mass spectrometry was performed using TripleTOF® 6600+ System. The spray voltage of the spectrometer was set at −4500 V, the turbo capillary temperature was set at 500 °C, the declustering potential (DP) was set at −80 V, collision energy (CE) was set at −10 eV, nebulizer gas (Gas 1) was set at 20 psi; heater gas (Gas 2) was set at 10 psi, and the curtain gas was set at 25 psi.

2.6. Detection of L-DOPA by an in-vitro method

The optimal conditions are used to test the reaction time of SsDDO protein and L-DOPA to generate CHAPCA. The reaction solution contains 62.5 mM sodium phosphate buffer at pH 8.0, 16.5 μM SsDDO, 1 mM $FeSO_4$, AA 10 mM, and 100 μM L-DOPA, every reaction 20 min, the characteristic absorption peak of CHAPCA at 414 nm was measured with a plate reader.

2.7. Detection of L-DOPA by cell-based method

Cells were diluted in M9 medium and incubated at 250 rpm, 37 °C (~O.D.600 = 0.4). The cells were induced with 100 μM IPTG and various concentrations of L-DOPA (0, 1, 5, 25, 75, and 125 μM). The mixtures were reacted at 37 °C for 30 min to allow enzymatic conversion of L-DOPA to CHAPCA. The addition of MABA to a medium lead to the production of CHAPCA-MA.

2.8. Paper-based analytical device

A Xerox Solid Ink Color Wax Printer (colorQube 8560dn, Fuji, Japan) was used to print hollow circles with an internal diameter at 4 mm and the line width of 0.2 mm. The wax-patterned paper was heated at 120 °C for 10 min for the wax to completely penetrate through paper substrate. The step of surface modification, 0.5% chitosan (0.05g chitosan dissolve in 2% of 10 mL acetic acid) was applied on the hydrophilic well of the paper substrate.

2.9. Sequential detection of dopamine and L-DOPA in a mixed solution

The solution containing 25 μM dopamine alone and dopamine with L-DOPA (100 and 500 μM) were examined. We next added resorcinol (1 mM) and Na_2CO_3 (50 mM) in mixed solutions, respectively. Resorcinol reacted with dopamine in the solution for 5 min to generate azamonardine. The fluorescence intensity (a.u.) was measured (excitation/emission: 360/485 nm) for the detection of dopamine. Next, the solution of above reaction and the solution containing L-DOPA alone were incubated with cells expressing SsDDO enzyme for 30 min to generate CHAPCA, and then MABA was added to form CHAPCA-MA with red fluorescence signal. Azamonardine and CHAPCA-MABA could be detected in the mixed sample using the cyan and red fluorescence emission.

3. Results and discussion

3.1. Characterization of SsDDO and optimization of protein-based biosensor

According to the biochemical study, SsDDO is octahedrally coordinated with a non-heme iron by two histidine residues, a glutamate residue, and three water molecules [30]. This structure provides a cavity containing the catalytic center for selective binding of L-DOPA. Next, the oxidative cleavage of L-DOPA forms linear semialdehyde (AHMS, a transient species, λ_{max} 375 nm), and cyclizes to a 3,4-dihydropyrrole-2-carboxylic acid (CHAPCA, λ_{max} 414 nm). SsDDO enzyme was purified from *E. coli* cells (Fig. S1). Enzyme activities were determined by absorption spectrum through the increase of λ_{max}, indicative of the production of CHAPCA.

We thus developed a colorimetric assay based on the formation of CHAPCA. Reaction conditions were optimized in terms of pH, co-factor selection, temperature, and reaction time. We first prepared buffer solutions with pH values of 6.2, 7.0, 7.5, 8.0, 8.5, and 9.0 for enzyme activity test. A reaction solution was prepared using purified protein (SsDDO), 0.5 mM $FeSO_4$, and 100 μM L-DOPA. The mixed solution was allowed to react for 40 min before measurement of the absorption spectrum. As shown in (Fig. 1A), absorbance was stronger in samples with a pH at 8; however, the activity significantly decreased in higher pH values. The absorbance peak at 414 nm is consistent with the reaction product CHAPCA, and AHMS is not observable under steady-state conditions, which is consistent with previous studies [34]. Note that iron ions with different valences can also affect the progress of the oxidation ring-opening reaction; therefore, we tested four iron salts as co-factors (Fig. 1B). Absorption intensity values revealed that ferrous ion is more conducive to the reactions than is a ferric ion. Overall, $FeSO_4$ was identified as the best co-factor for the reaction between SsDDO and L-DOPA. These results were consistent with previous observations that SsDDO employs a Fe(II) to catalyze the insertion of dioxygen into the aromatic ring of L-DOPA. Experimental results revealed only negligible differences in the absorption intensity values of CHAPCA generated at different temperatures (Fig. 1C), indicating great thermal stability of SsDDO. With the CHAPCA synthesis reaction temperature fixed at 37 °C, we monitored λ_{414} intensity at a 5 min interval over the course of the reaction (Fig. 1D). The intensity initially increased, reaching a plateau within roughly 30 min.

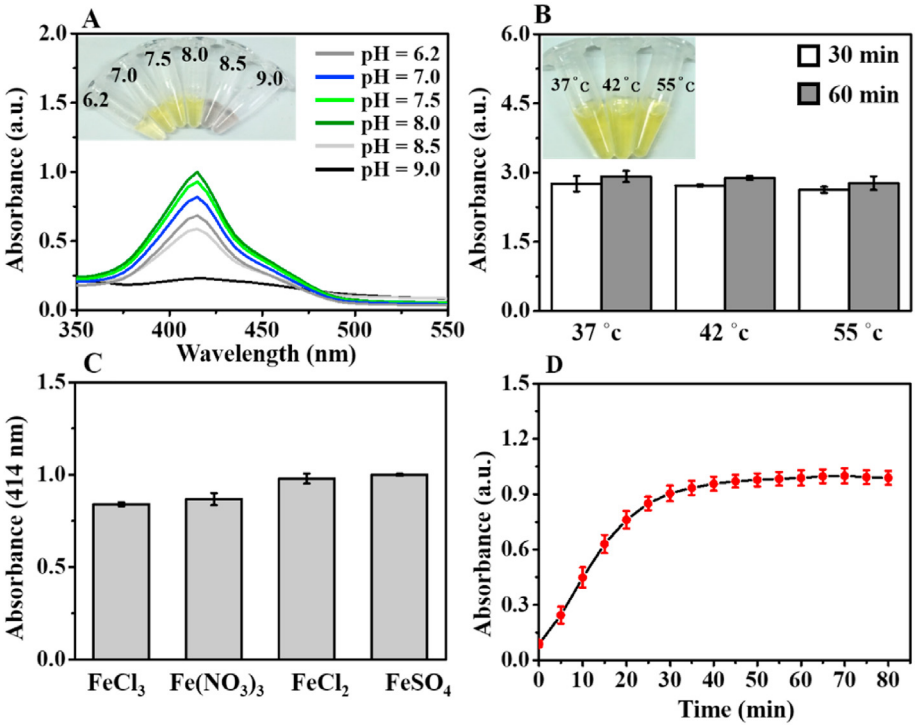

Fig. 1. Activity test of SsDDO, the concentration of L-DOPA is fixed at 125 μM in all experiments (A) Test the activity of SsDDO enzyme in phosphate buffer solutions of different pH values (pH 6.2, 7.0, 7.5, 8.0, 8.5, and 9.0). (B) Test the reactivity of SsDDO enzyme at different temperatures (37, 42 and 55 °C). (C) The effect of using different iron ions ($FeCl_3$, $Fe(NO_3)_3$, $FeCl_2$, $FeSO_4$) on the synthesis of CHAPCA. (D) Absorption spectrum over reaction time-course of SsDDO enzyme in the presence of L-DOPA.

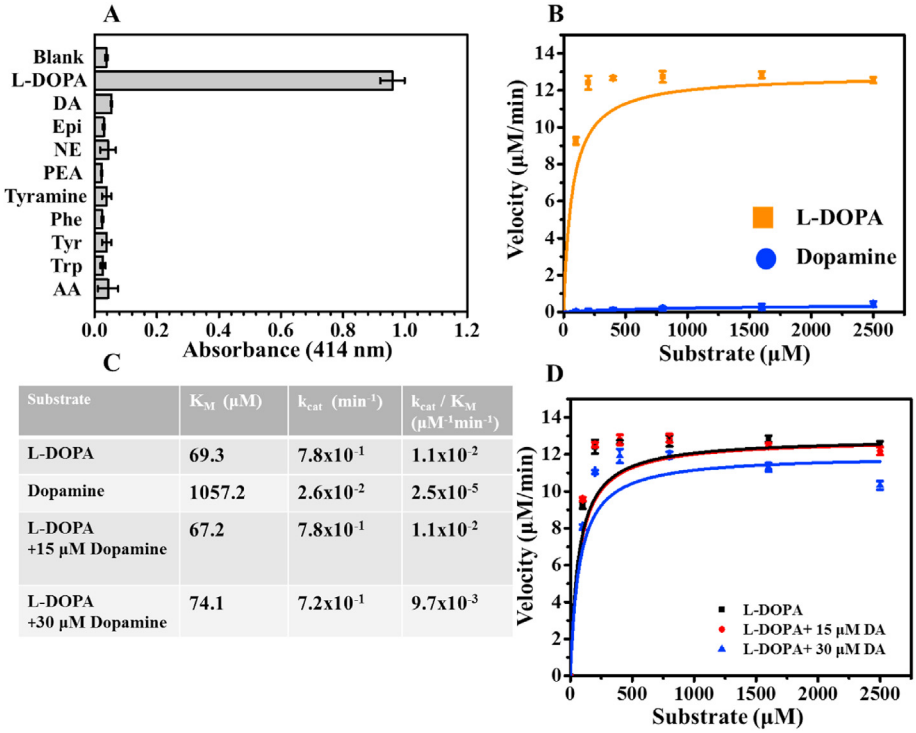

Substrate	K_M (μM)	k_{cat} (min^{-1})	k_{cat} / K_M ($\mu M^{-1}min^{-1}$)
L-DOPA	69.3	$7.8x10^{-1}$	$1.1x10^{-2}$
Dopamine	1057.2	$2.6x10^{-2}$	$2.5x10^{-5}$
L-DOPA +15 μM Dopamine	67.2	$7.8x10^{-1}$	$1.1x10^{-2}$
L-DOPA +30 μM Dopamine	74.1	$7.2x10^{-1}$	$9.7x10^{-3}$

Fig. 2. (A) Specificity of the purified SsDDO in the presence of various substrates including L-DOPA, DA, Epi, NE, PEA, tyramine, Phe, Tyr, Trp, and AA (at a concentration of 125 μM) (B) Reaction kinetics of SsDDO with L-DOPA or dopamine at various concentrations. Rates of increase at 414 nm for CHAPCA were plotted. (C) Summary of Michaelis constant (K_M), catalytic constant (k_{cat}), and catalytic efficiency (k_{cat}/K_M) values. (D) Reaction kinetics of SsDDO with L-DOPA in the presence of dopamine at 15 and 30 μM.

3.2. Substrate specificity and interference effects of dopamine

Experiments were also conducted to determine the specificity of SsDDO in the presence of catecholamines and metabolite intermediates such as DA, Epi, NE, PEA, tyramine, Phe, Tyr, Try, and AA (at a concentration of 125 μM) (Fig. 2A). The relative λ_{414} intensity toward L-DOPA after reacting with the SsDDO enzyme was plotted. None of the potentially-interfering substances generated signals exceeding 0.08 units, thereby demonstrating the outstanding specificity of SsDDO to the oxidation ring-opening reaction of L-DOPA. The affinity between SsDDO and L-DOPA was examined by enzyme kinetic measurements (Fig. 2B). We examined the reaction rate and specificity using the Michaelis–Menten kinetics method. The rate of L-DOPA conversion to CHAPCA depended on the concentrations of the enzyme as well as the substrate. Increasing the concentration of either the enzyme or L-DOPA was shown to increase the reaction rate. Kinetic analysis was performed by monitoring the concentration CHAPCA by varying the L-DOPA concentration under a constant SsDDO enzyme concentration. We calculated the values of Michaelis constant (K_M), catalytic constant (k_{cat}), and catalytic efficiency (k_{cat}/K_M) by fitting the steady-state rates to the Michaelis–Menten equation based on the formation of CHAPCA (Fig. 2C). These results indicate that the SsDDO demonstrated much stronger affinity (K_M) toward L-DOPA compared with dopamine, i.e. the other common substrate of DOPA dioxygenases. Notably, dopamine with SsDDO had a 2000 fold lower k_{cat}/K_M than L-DOPA, demonstrating that L-DOPA is a better substrate for SsDDO. The enzyme inhibition assay was performed to evaluate the interference of dopamine (Fig. 2D). These results suggest that free dopamine, which acts closely as a mimic competitive inhibitor (K_M increases and v_{max} decreases, Fig. 2C) with respect to L-DOPA, binds SsDDO in a similar active site.

We next sought to use SsDDO enzyme to examine the specificity for recognition of L-DOPA in the presence of dopamine. We therefore conducted an additional experiment with the dopamine concentration fixed at 50 μM and adjusted the L-DOPA concentration to 50 or 100 μM before detecting the λ_{414} intensity (Fig. S2). Our results revealed that when the mixed solution reacted, the absorption intensity was close to that with L-DOPA alone, thereby demonstrating that the presence of dopamine did not have a significant effect on L-DOPA sensing performance.

We then investigated the efficacy of SsDDO in the detection of L-DOPA in terms of color change under the above conditions. When L-DOPA was added to the reaction solution, an increases in the production CHAPCA was observed (Fig. 3A). Overall, the intensity increased with an increase in L-DOPA concentration (Fig. 3B) presents a favorable linear relationship (R^2 = 0.997) with the detection limit at 2.11 μM, and the inset photograph shows the production of CHAPCA (colorless to yellow) in reactions containing L-DOPA. In the absence of L-DOPA, no color changes can be observed, indicating color changes specifically attributed to the enzymatic reactions.

3.3. Cell-based biosensor for the detection of L-DOPA

We investigate the possibility for rapid detection of L-DOPA using whole-cell sensors (*E. coli* expressing the SsDDO). Cells were grown in M9 medium until reaching the OD = 0.4–0.6 logarithmic growth period. We then added IPTG to induce expression of the SsDDO protein. Finally, we added L-DOPA at various concentrations to the bacterial culture medium with various incubation intervals, before measuring the absorption intensity. A visually detectable signal amplification was observed after incubating the cells in the presence of L-DOPA for 10 min (inset in Fig. S3). The dose-response studies between of L-DOPA concentrations and λ_{414} was carried out and presented in (Fig. S3). Compared with the purified SsDDO protein, whole-cell sensing required only 10 min to obtain a detectable signal with a good linear range and the comparable detection limit (2.29 μM).

3.4. Derivatization of CHAPCA with MABA

Next, CHAPCA was incubated with 17 amines to further derivatize CHAPCA in the formation of compounds with red fluorescence. To determine completeness of the reaction, we recorded the fluorescence spectrum and performed color analysis of white light and fluorescent images (Fig. 4A and B). Most amines incubating with CHAPCA pigments did not show a notable change in color (Fig. 4B). Our experiment results revealed that in this series of amines, the MABA compound presented the red fluorescent signal with the highest intensity after reaction with CHAPCA (Fig. 4A). MABA and CHAPCA pigments underwent a 1,4-addition reaction with the color of the solution changing from yellow to orange-red, indicating the generation of red fluorescent pigments (Fig. S4A). The red color of the fluorescent signal can be attributed to the fact that aromatic compounds undergo low-energy π-π* transitions leading to the generation of fluorescent signals and amines with non-bonded electron pairs enhance the intensity of fluorescent signals. We validated the production of CHAPCA and 4-(3-carboxy-1-((3-carboxyphenyl)amino)-3-oxopropyl)-2,3-dihydro-1H-pyrrole-2-carboxylic acid (CHAPCA-MABA) by collecting bacterial supernatant from the cell culture via centrifuge, and analyzing the

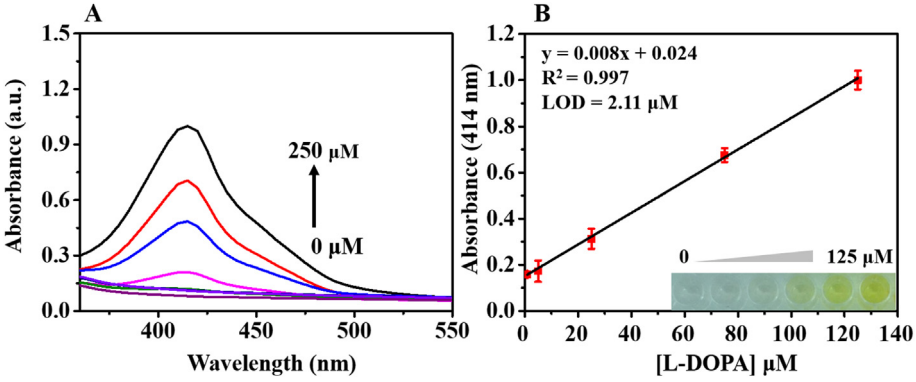

Fig. 3. (A) Absorption spectrum of reaction solutions containing L-DOPA at various concentrations (0, 1, 5, 25, 75, and 125 μM). (B) The intensity of λ_{414} was observed as a linear function of concentrations of L-DOPA. Linear ranges for L-DOPA were 1–125 μM, and LOD was 2.11 μM. Inset: the corresponding photographs in the presence of L-DOPA at various concentrations.

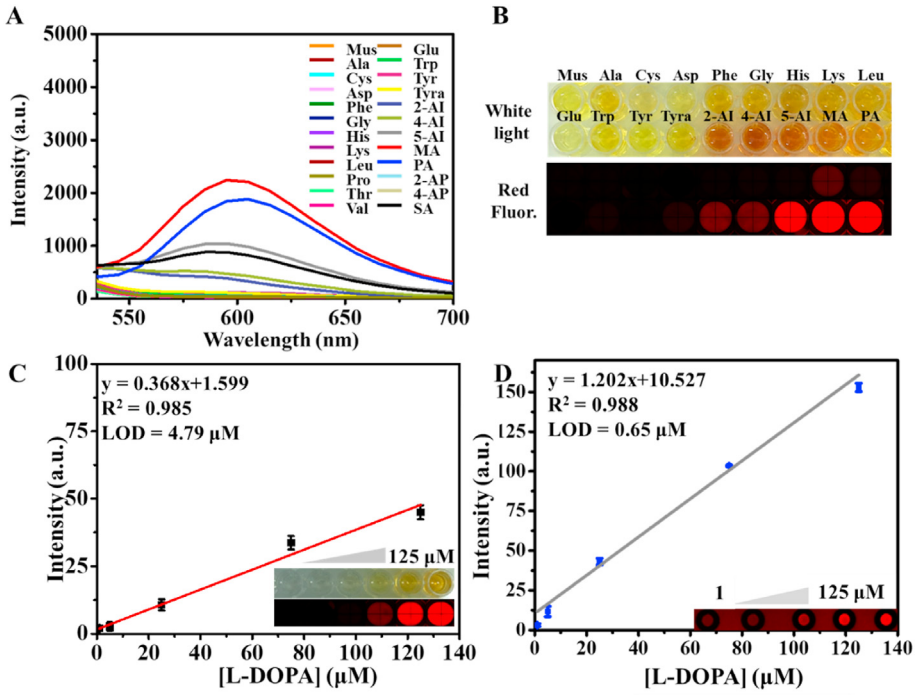

Fig. 4. (A) Fluorescence emission spectroscopy of CHAPCA after incubating with various amines at 30 mM including (CHAPCA, alanine, cysteine, aspartate, phenylalanine, glycine, histidine, lysine, leucine, glutamic acid, tryptophan, tyrosine, tyramine, 2-aminoterephthalic acid, 4-aminoterephthalic acid, 5-aminoterephthalic acid, 3-aminobenzoic acid, and 4-aminobenzoic acid). (B) The white light and red fluorescence photograph from (A). Red fluorescence intensity of CHAPCA-MABA (C) in solution and (D) on paper with 0.5% chitosan modification the presence of various concentrations of L-DOPA. (For interpretation of the references to color in this figure legend, the reader is referred to the Web version of this article.)

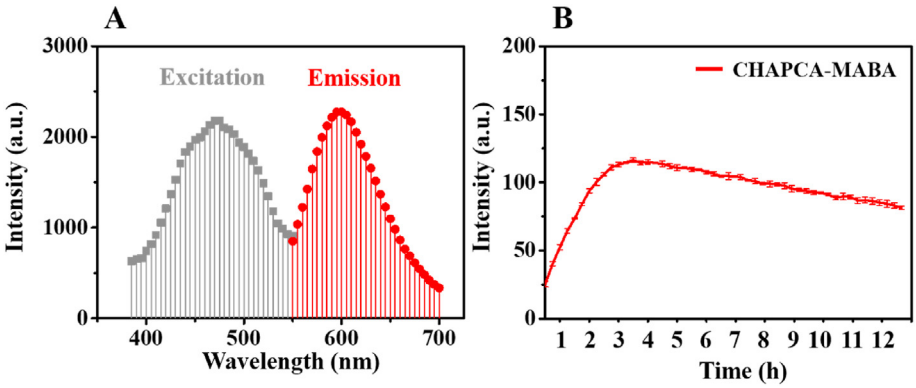

Fig. 5. (A) The emission and excitation spectrum of CHAPCA-MABA. (B) Time-course of the production of CHAPCA-MABA (measured by fluorescence of CHAPCA-MABA).

supernatant through high-resolution electrospray mass spectrometry (Fig. S4B and Fig. S4C). A similar resulting compound was obtained when (4-aminobenzoic acid, PABA) was incubated with CHAPCA (Fig. S4D).

We examined the fluorescence spectra to investigate the optical properties of CHAPCA-MABA. The CHAPCA-MABA exhibited red emissions at approximately 600 nm upon excitation maximum at 475 nm (Fig. 5A). We also examined the reaction time-course through the fluorescence signals of CHAPCA-MABA at various time intervals. The intensity of the CHAPCA-MABA achieved the maximum signal intensity at 3 h (Fig. 5B). However, for rapid L-DOPA detection, red fluorescence associated with the CHAPCA-MABA compound is recorded at 1 h. As shown in (Fig. 4C) the intensity of the red fluorescence increased proportionally with the concentration of L-DOPA, indicating that CHAPCA-MABA formation is dependent on the concentration of L-DOPA with the detection limit of 4.79 μM. For the rapid and sensitive detection of L-DOPA at a low cost, we sought to examine the colorimetric reaction on a paper-based analytical device. The final reaction solution from the whole-cell sensing was directly spotted on the filter paper. Interestingly, paper modified with 0.5% chitosan, a natural biopolymer, significantly enhanced the fluorescence signals (FigS. S5A and B). As the concentration of L-DOPA was increased from the range of 1–125 μM, we observed a gradual increase in red fluorescence intensity with a limit of detection at 0.65 μM (Fig. 4D), which is ten times better than that in solution. These results suggest paper-based analytical device presents a better sensitivity after surface modification by chitosan, which meets the clinical requirements for the monitoring of L-DOPA in Parkinson's patients. In previous reports [38], the peak plasma concentrations of L-DOPA in the blood of Parkinson's disease patients on L-DOPA therapy ranges from 1.26 to 12.27 μM [39, 40].

Table 1
Real sample analysis.

Sample	Determination of L-DOPA in real samples			
	Spiked (μM)	Found (μM)	Recovery (% n = 3)	RSD (% n = 3)
Protein-based	125	132.9	106.3	9.93
	75	99.0	117.4	17.80
Cell-based	125	117.4	93.5	4.80
	75	75.4	100.5	4.43

Despite the outstanding results obtained of the laboratory aqueous L-DOPA solutions, the applicability of the sensor strictly depends on selective recognition in complex bio-fluids. L-DOPA is commonly quantified in serum to monitor or assist in the preparation and administration of medication. To determine the reactivity of the enzyme in the serum matrix, we used the standard addition method (spiking L-DOPA to fetal bovine serum, FBS) to detect L-DOPA concentrations based on absorption values. Commercial FBS was used as a sample matrix. We sought to reduce the effect of the serum matrix on CHAPCA absorption by diluting it to 30%. In the experiments, the recovery rate was 106–117% in the detection of L-DOPA. We also tested the detection of L-DOPA in 30% FBS using the cell-based detection method. As shown in Table 1, the recovery rates were ranging from 93 to 101% and RSDs were less than 5%.

L-DOPA, a dopaminergic precursor, is often used to restore the reduction of dopamine. We thus sought to determine the level of dopamine simultaneously. The method used for dopamine was modified from the protocol outlined in a previous study [31–33]. Briefly, it involves the selectively coupling reaction between dopamine and resorcinol in an alkaline environment to generate a fluorescent azamonardine. The color of the solution was yellow with a characteristic absorption wavelength of 420 nm (inset, Fig. 6A). The increase in intensity moved toward linearity as the concentration of dopamine was increased, and the lowest detection limit was 1.23 μM (Fig. 6A). The fluorescence intensity of azamonardine at wavelengths of 485 nm increased with the concentration of dopamine as well (Fig. 6B) with a detection limit of 1.06 μM. Furthermore, the proposed fluorescence strategy shows promising potential for the selective assaying dopamine without interference from other structural analogs (Fig. 6C). A better limit of detection on a paper-based device with chitosan modification was again observed compared to those results in solution or on a paper without modification (Fig. 6D and S5B).

Thus, we sought to develop a novel approach to the detection of dopamine and L-DOPA via a stepwise reaction. The mixed sample containing dopamine and L-DOPA is firstly reacted with resorcinol for 5 min generating the cyan-fluorescent compound. The concentration of dopamine in the mixed sample could be determined using the cyan fluorescence intensity. Next, the whole-cell sensors expressing SsDDO were added to the mixed sample to react with the remaining L-DOPA. After the production of yellow CHAPCA pigment, we added MABA to produce the red fluorescent compound CHAPCA-MABA. The concentration of L-DOPA in the mixed sample can be measured from this reaction by the emission spectra of azamonardine and CHAPCA-MABA (Fig. 7A).

To validate the proposed approach, we examined the interference of the co-existence of dopamine and L-DOPA. In the first step, we detected the formation of azamonardine in the solution containing dopamine (25 μM) alone, and the solution containing dopamine (25 μM) and L-DOPA (100 and 500 μM). The resorcinol was added to the above solution over a period of 5 min. The measured fluorescence intensity was close to that of dopamine alone, thereby demonstrating that the presence of L-DOPA did not affect dopamine detection results. In the second step, the detection of the L-DOPA was validated in the mixed sample (Fig. 7B). We added the whole-cell sensor in the solution from the above

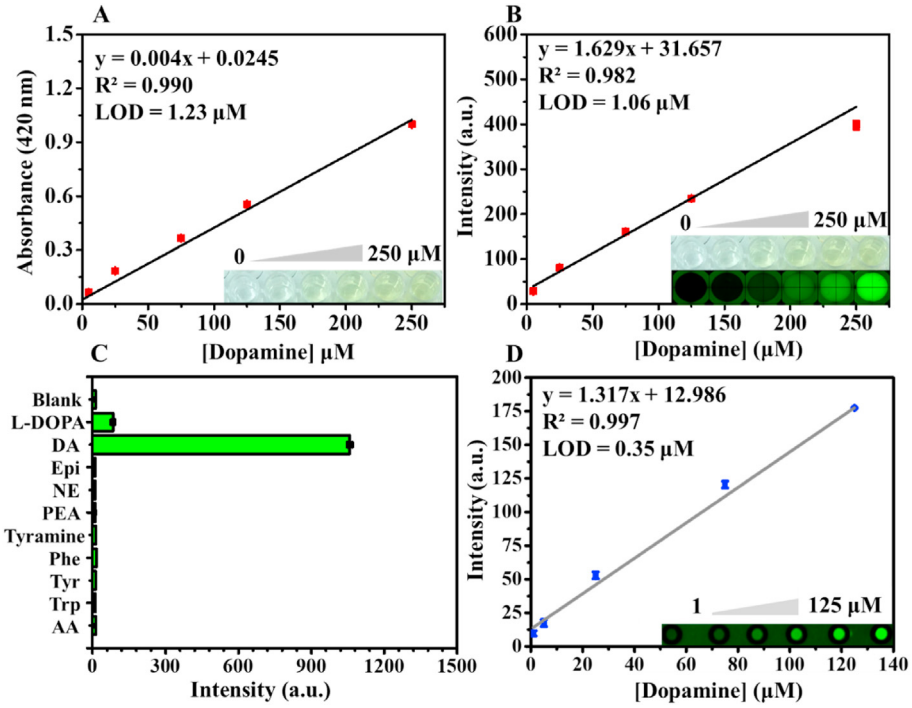

Fig. 6. Azamonardine (λ_{max} 420 nm) formation in the presence of various concentrations of dopamine. The relationship between (A) absorption intensity at 420 nm (B) fluorescence intensity (ex/em: 360/485 nm) and various dopamine concentrations (1, 5, 25, 75, 125, 250 μM). The reaction time is 5 min. Inset: the white light photos of the coupling reaction between dopamine and resorcinol under different dopamine concentrations. (C) The fluorescence of the resorcinol reaction in the presence of various substrates including L-DOPA, DA, Epi, NE, PEA, tyramine, Phe, Tyr, Trp, and AA (at a concentration of 125 μM). (D) The same experiments were carried out on paper with 0.5% chitosan modification.

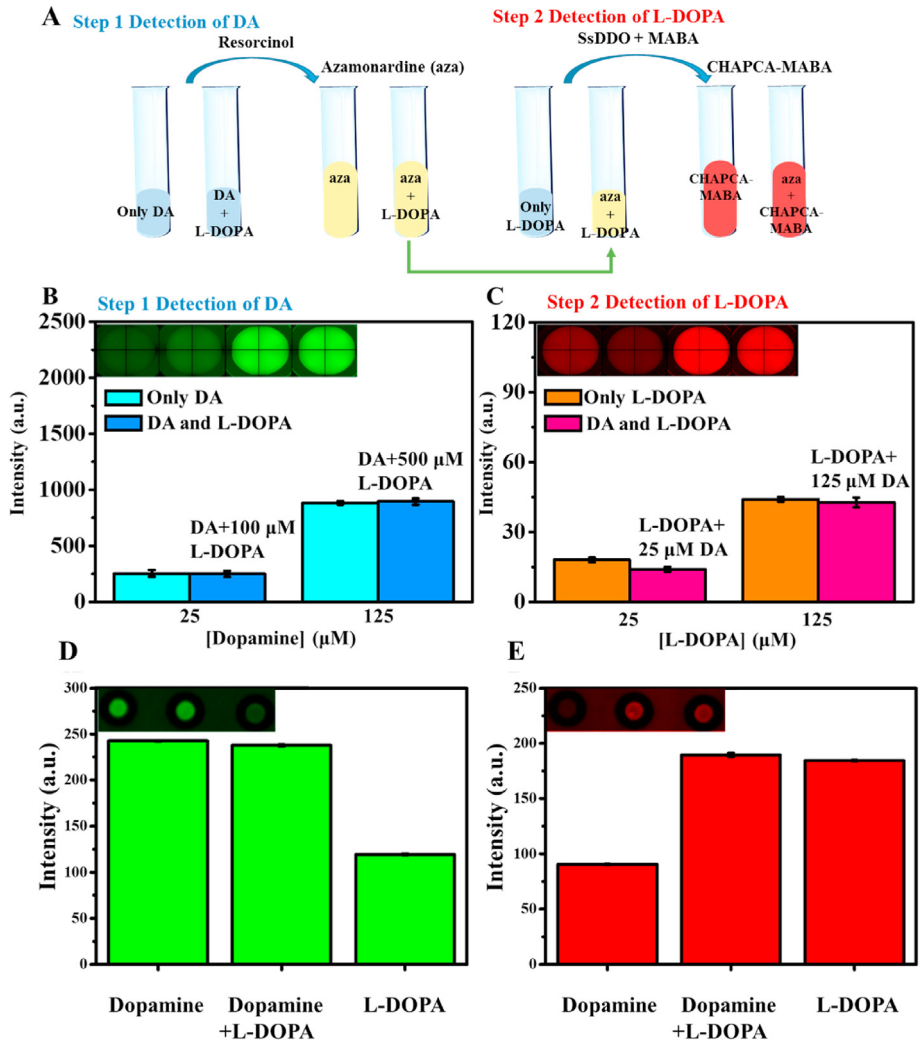

Fig. 7. A novel approach to detecting dopamine and L-DOPA via a stepwise reaction. (A) The mixed sample containing dopamine (25 and 125 μM) and L-DOPA (100 and 500 μM) is firstly reacted with resorcinol for 5 min generating the cyan-fluorescent compound (azamonardine). (B) The measured fluorescence intensity of dopamine alone and the mixed sample. We added the whole-cell sensor in the solution from the above reaction. The unreacted L-DOPA in the mixture will react with the SsDDO. (C) The measured fluorescence intensity of L-DOPA alone and the mixed sample. A stepwise reaction on chitosan-modified paper. (D) The measured fluorescence intensity of samples by reacting dopamine (125 μM), L-DOPA (125 μM), and a mixture of two with resorcinol. (E) The measured fluorescence intensity of samples by reacting dopamine (125 μM), L-DOPA (125 μM), and the mixture of two with the whole-cell sensors and MABA. (For interpretation of the references to color in this figure legend, the reader is referred to the Web version of this article.)

reaction. The unreacted L-DOPA in the mixture will react with the SsDDO. The red fluorescent signal generated by CHAPCA-MABA was measured at 590 nm. In experiments, the measured fluorescence intensity of the mixed solution was close to that of the solution containing L-DOPA alone, thereby demonstrating that the presence of azamonardine and un-reacted resorcinol in the mixed samples did not affect the formation of CHAPCA-MABA (Fig. 7C). We again examined the same reaction on a paper-based analytical device (Fig. 7D and E). Similar fluorescent signals were obtained in mixed solution and single analyte alone, indicating the robustness of the purposed stepwise reaction.

4. Conclusions

In summary, SsDDO, a thermal stable enzyme, was used for the selective detection of L-DOPA for the first time. Previously, we have expressed DOPA dioxygenase from *Mirabilis jalapa* (plant) for the detection of dopamine and L-DOPA [35]. The enzyme can use both L-DOPA and dopamine as substrates to form yellow pigment, which makes it impossible to determine L-DOPA in the co-presence of dopamine. In the present study, the SsDDO enzyme shows a greater specificity toward L-DOPA (with 2000 higher k_{cat}/K_M). By using cell-based assays, it could serve as a high-throughput screening platform to assay samples in relatively short amount of time. Additionally, a sequential analysis method to detect the coexistence of dopamine and L-DOPA with a high degree of sensitivity using the dual-color fluorescent signals from azamonardine and CHAPCA-MABA was developed. The experiment results clearly show that the analytical performance of current method is comparable with that of other reported L-DOPA/dopamine sensing devices (Tables S1 and 2). Paper microfluidic platforms modified with chitosan were applied for fast and cost-effective analysis of dopamine and L-DOPA in the mixed solutions, with a limit of detection of (L-DOPA: 580 nM and dopamine: 345 nM), which meets the clinical requirements for the monitoring of L-DOPA/dopamine in Parkinson's patients. In conclusion, the purposed platform has outstanding potential for rapid and high-throughput quantitative analysis with economical reagents, which can be perfectly used for the future analytical applications in the detection of L-DOPA in biological samples co-existing with dopamine.

CRediT authorship contribution statement

Chia-Wen Chang: Data curation, Visualization, Investigation. **Yu-Hsuan Lin:** Data curation, Visualization, Conceptualization, Methodology. **Cheng-Han Tsai:** Data curation, Visualization, Investigation. **Sivasankar Kulandaivel:** Writing – original draft, preparation. **Yi-Chun Yeh:** Conceptualization, Methodology, Writing – review & editing.

Declaration of competing interest

The authors declare that they have no known competing financial interests or personal relationships that could have appeared to influence the work reported in this paper.

Acknowledgments

This work was funded by the Ministry of Science and Technology of Taiwan under the project number 107-2113-M-003-013-MY3 and 110-2113-M-003-009-. Dr. Sivasankar Kulandaivel gratefully acknowledges Ministry of Science and Technology, Taiwan for the postdoctoral fellowship (110-2811-M-003-512-). This work also was financially supported by the National Taiwan Normal University within the framework of the Higher Education Sprout Project by the Ministry of Education in Taiwan.

Appendix A. Supplementary data

Supplementary data to this article can be found online at https://doi.org/10.1016/j.aca.2022.339641.

References

[1] F. Lanau, M.T. Zenner, O. Civelli, D.S. Hartman, Epinephrine and norepinephrine act as potent agonists at the recombinant human dopamine D4 receptor, J. Neurochem. 68 (1997) 804–812.
[2] W.J. Burke, S.W. Li, H.D. Chung, D.A. Ruggiero, B.S. Kristal, E.M. Johnson, P. Lampe, V.B. Kumar, M. Franko, E.A. Williams, Neurotoxicity of MAO metabolites of catecholamine neurotransmitters: role in neurodegenerative diseases, Neurotoxicology 25 (2004) 101–115.
[3] M.D. De Bellis, A.S. Baum, B. Birmaher, M.S. Keshavan, C.H. Eccard, A.M. Boring, F.J. Jenkins, N.D. Ryan, Developmental traumatology part I: biological stress systems, Biol. Psychiatr. 45 (1999) 1259–1270.
[4] C. Mehler-Wex, P. Riederer, M. Gerlach, Dopaminergic dysbalance in distinct basal ganglia neurocircuits: implications for the pathophysiology of Parkinson's disease, schizophrenia and attention deficit hyperactivity disorder, Neurotox. Res. 10 (2006) 167–179.
[5] L. Salerno, S. Ramat, G. Solari, G. Grassi, S. Pallanti, Parkinson's disease with impulse control disorders: higher prevalence (frequency) of symptoms of attention deficit hyperactivity disorder, Int J Clin Psychiatr. 7 (2019) 1–7.
[6] D. Merims, N. Giladi, Dopamine dysregulation syndrome, addiction and behavioral changes in Parkinson's disease, Park. Relat. Disord. 14 (2008) 273–280.
[7] J. Dutton, L.G. Copeland, J.R. Playfer, N.B. Roberts, Measuring L-dopa in plasma and urine to monitor therapy of elderly patients with Parkinson disease treated with L-dopa and a dopa decarboxylase inhibitor, Clin. Chem. 39 (1993) 629–634.
[8] H. Heikkinen, A. Varhe, T. Laine, J. Puttonen, M. Kela, S. Kaakkola, K. Reinikainen, Entacapone improves the availability of L-dopa in plasma by decreasing its peripheral metabolism independent of L-dopa/carbidopa dose, Br. J. Clin. Pharmacol. 54 (2002) 363–371.
[9] T. Nagatsu, M. Sawada, L-dopa therapy for Parkinson's disease: past, present, and future, Park. Relat. Disord. 15 (2009) S3–S8.
[10] R.M. Riggin, R.L. Alcorn, P.T. Kissinger, Liquid chromatographic method for monitoring therapeutic concentrations of L-dopa and dopamine in serum, Clin. Chem. 22 (1976) 782–784.
[11] C. Muzzi, E. Bertocci, L. Terzuoli, B. Porcelli, I. Ciari, R. Pagani, R. Guerranti, Simultaneous determination of serum concentrations of levodopa, dopamine, 3-O-methyldopa and α-methyldopa by HPLC, Biomed. Pharmacother. 62 (2008) 253–258.
[12] A.H.V. Schapira, C.W. Olanow, Drug selection and timing of initiation of treatment in early Parkinson's disease, Ann. Neurol.: Off. J. Am. Neurol. Assoc. Child Neurol. Soc. 64 (2008) S47–S55.
[13] S. Shahrokhian, E. Asadian, Electrochemical determination of L-dopa in the presence of ascorbic acid on the surface of the glassy carbon electrode modified by a bilayer of multi-walled carbon nanotube and poly-pyrrole doped with tiron, J. Electroanal. Chem. 636 (2009) 40–46.
[14] G.S.S. Sunder, A. Rohanifar, A.M. Devasurendra, J.R. Kirchhoff, Selective determination of l-DOPA at a graphene oxide/yttrium oxide modified glassy carbon electrode, Electrochim. Acta 301 (2019) 192–199.
[15] Q. Wang, M.R. Das, M. Li, R. Boukherroub, S. Szunerits, Voltammetric detection of L-dopa and carbidopa on graphene modified glassy carbon interfaces, Bioelectrochemistry 93 (2013) 15–22.
[16] G. Cannazza, A. Di Stefano, B. Mosciatti, D. Braghiroli, M. Baraldi, F. Pinnen, P. Sozio, C. Benatti, C. Parenti, Detection of levodopa, dopamine and its metabolites in rat striatum dialysates following peripheral administration of L-DOPA prodrugs by mean of HPLC-EC, J. Pharm. Biomed. Anal. 36 (2005) 1079–1084.
[17] N. Satheeshkumar, M. Pradeepkumar, S. Shanthikumar, V.J. Rao, Development of validated stability indicating assay method for simultaneous estimation of metformin hydrochloride and vildagliptin by RP-HPLC, Drug Res. 64 (2014) 124–129.
[18] J. Coello, S. Maspoch, N. Villegas, Simultaneous kinetic-spectrophotometric determination of levodopa and benserazide by bi- and three-way partial least squares calibration, Talanta 53 (2000) 627–637.
[19] M. Grunhut, M.E. Centurion, W.D. Fragoso, L.F. Almeida, M.C. de Araujo, B.S. Fernandez Band, Flow-batch technique for the simultaneous enzymatic determination of levodopa and carbidopa in pharmaceuticals using PLS and successive projections algorithm, Talanta 75 (2008) 950–958.
[20] L. Zhang, G. Chen, Q. Hu, Y. Fang, Separation and determination of levodopa and carbidopa in composite tablets by capillary zone electrophoresis with amperometric detection, Anal. Chim. Acta 431 (2001) 287–292.
[21] S. Zhao, W. Bai, B. Wang, M. He, Determination of levodopa by capillary electrophoresis with chemiluminescence detection, Talanta 73 (2007) 142–146.
[22] S. Abbasi-Moayed, M.R. Hormozi-Nezhad, M. Maaza, A multichannel single-well sensor array for rapid and visual discrimination of catecholamine neurotransmitters, Sensor. Actuator. B Chem. 296 (2019) 126691.
[23] A.S. Saini, J. Kumar, J.S. Melo, Microplate based optical biosensor for l-Dopa using tyrosinase from Amorphophallus campanulatus, Anal. Chim. Acta 849 (2014) 50–56.
[24] H. Li, J. Liu, S. Guo, Y. Zhang, H. Huang, Y. Liu, Z. Kang, Carbon dots from PEG for highly sensitive detection of levodopa, J. Mater. Chem. B 3 (2015) 2378–2387.
[25] S. Scott, E.J. Behrman, A simple colorimetric assay for L-dopa in the presence of tyrosine using the phosphotungstic acid reagent, Anal. Lett. 21 (1988) 183–191.
[26] J.I. Routh, R.E. Bannow, R.W. Fincham, J.L. Stoll, Excretion of L-dopa and its metabolites in urine of Parkinson's disease patients receiving L-dopa therapy, Clin. Chem. 17 (1971) 867–871.
[27] K.L. Colabroy, I.R. Smith, A.H.S. Vlahos, A.J. Markham, M.E. Jakubik, Defining a kinetic mechanism for L-DOPA 2, 3 dioxygenase, a single-domain type I extradiol dioxygenase from Streptomyces lincolnensis, Biochim. Biophys. Acta Protein Proteonomics 1844 (2014) 607–614.
[28] K.L. Colabroy, A.D. Horwitz, V.R. Basciano, Y. Fu, K.M. Travitz, M.K. Robinson, B.A. Shimanski, T.W. Hoffmann, A new way of belonging: active-site investigation of L-DOPA dioxygenase, a VOC family enzyme from lincomycin biosynthesis, Biochemistry 58 (2019) 4794–4798.
[29] K.L. Colabroy, Tearing down to build up: metalloenzymes in the biosynthesis lincomycin, hormaomycin and the pyrrolo [1, 4] benzodiazepines, Biochim. Biophys. Acta Protein Proteonomics 1864 (2016) 724–737.
[30] Y. Wang, I. Shin, Y. Fu, K.L. Colabroy, A. Liu, Crystal structures of L-DOPA dioxygenase from Streptomyces sclerotialus, Biochemistry 58 (2019) 5339–5350.
[31] X. Zhang, Y. Zhu, X. Li, X. Guo, B. Zhang, X. Jia, B. Dai, A simple, fast and low-cost turn-on fluorescence method for dopamine detection using in situ reaction, Anal. Chim. Acta 944 (2016) 51–56.
[32] P. Ni, C. Chen, Y. Jiang, C. Zhang, B. Wang, Y. Lu, H. Wang, A fluorescent assay for alkaline phosphatase activity based on inner filter effect by in-situ formation of fluorescent azamonardine, Sensor. Actuator. B Chem. 302 (2020) 127145.
[33] M.L. Alfieri, L. Panzella, S.L. Oscurato, M. Salvatore, R. Avolio, M.E. Errico, P. Maddalena, A. Napolitano, V. Ball, M. d'Ischia, Hexamethylenediamine-mediated polydopamine film deposition: inhibition by resorcinol as a strategy for mapping quinone targeting mechanisms, Front. Chem. 7 (2019) 407.
[34] K.L. Colabroy, I.R. Smith, A.H.S. Vlahos, A.J. Markham, M.E. Jakubik, Defining a kinetic mechanism for l-DOPA 2,3 dioxygenase, a single-domain type I extradiol dioxygenase from Streptomyces lincolnensis, Biochim. Biophys. Acta Protein Proteonomics 1844 (2014) 607–614.
[35] Y.-K. Lin, Y.-C. Yeh, Dual-signal microbial biosensor for the detection of dopamine without inference from other catecholamine neurotransmitters, Anal. Chem. 89 (2017) 11178–11182.